

**First-order phase transition in a majority-vote model with inertia**Hanshuang Chen,<sup>1,\*</sup> Chuansheng Shen,<sup>2,3</sup> Haifeng Zhang,<sup>4</sup> Guofeng Li,<sup>1</sup> Zhonghuai Hou,<sup>5,†</sup> and Jürgen Kurths<sup>2,6,‡</sup><sup>1</sup>*School of Physics and Materials Science, Anhui University, Hefei 230601, China*<sup>2</sup>*Department of Physics, Humboldt University, 12489 Berlin, Germany*<sup>3</sup>*Department of Physics, Anqing Normal University, Anqing 246011, China*<sup>4</sup>*School of Mathematical Science, Anhui University, Hefei 230601, China*<sup>5</sup>*Hefei National Laboratory for Physical Sciences at the Microscale and Department of Chemical Physics, University of Science and Technology of China, Hefei 230026, China*<sup>6</sup>*Potsdam Institute for Climate Impact Research, 14473 Potsdam, Germany*

(Received 28 January 2016; revised manuscript received 10 February 2017; published 10 April 2017)

We generalize the original majority-vote model by incorporating inertia into the microscopic dynamics of the spin flipping, where the spin-flip probability of any individual depends not only on the states of its neighbors, but also on its own state. Surprisingly, the order-disorder phase transition is changed from a usual continuous or second-order type to a discontinuous or first-order one when the inertia is above an appropriate level. A central feature of such an explosive transition is a strong hysteresis behavior as noise intensity goes forward and backward. Within the hysteresis region, a disordered phase and two symmetric ordered phases are coexisting and transition rates between these phases are numerically calculated by a rare-event sampling method. A mean-field theory is developed to analytically reveal the property of this phase transition.

DOI: [10.1103/PhysRevE.95.042304](https://doi.org/10.1103/PhysRevE.95.042304)**I. INTRODUCTION**

Phase transitions in ensembles of complex networked systems have been a subject of intense research in statistical physics and many other disciplines [1]. These results are of fundamental importance for understanding various dynamical processes in the real world, such as percolation [2,3], epidemic spreading [4], synchronization [5,6], and collective phenomena in social networks [7].

Discontinuous or explosive transitions in complex networks have received growing attention since the discovery of an abrupt percolation transition in random networks [8,9] and scale-free networks [10,11]. Later studies affirmed that this transition is actually continuous but with an unusual finite-size scaling [12–14], yet many related models show truly discontinuous and anomalous transitions (see [15] for a recent review). Strikingly different from continuous phase transitions, in an explosive (or a first-order) phase transition an infinitesimal increase of the control parameter can give rise to a considerable macroscopic effect. Subsequently, an explosive phenomenon was found in the dynamics of cascading failures in interdependent networks [16–18], in contrast to the second-order continuous phase transition found in isolated networks. More recently, such explosive phase transitions have been reported in various systems, such as explosive synchronization due to a positive correlation between the degrees of nodes and the natural frequencies of the oscillators [19–21] or an adaptive mechanism [22], discontinuous percolation transition due to an inducing effect [23], spontaneous recovery [24], and explosive epidemic outbreak due to cooperative coinfections of multiple diseases [25–27].

In this paper we report a first-order order-disorder phase transition in a generalized majority-vote (MV) model by incorporating the effect of individuals' inertia (called the inertial MV model). The MV model is one of the simplest nonequilibrium generalizations of the Ising model that displays a continuous order-disorder phase transition at a critical value of noise [28]. It has been extensively studied in the context of complex networks, including random graphs [29,30], small-world networks [31–33], and scale-free networks [34,35]. However, the continuous nature of the order-disorder phase transition is not affected by the topology of the underlying networks [36]. In our model we have included a substantial change to make it more realistic, namely, the state update of each node depends not only on the states of its neighboring nodes, but also on its own state. In fact, in a social or biological context individuals have a tendency for beliefs to endure once formed. In a recent experimental study, behavioral inertia was found to be essential for collective turning of starling flocks [37]. We refer this modification as the inertial effect. Surprisingly, we find that as the level of the inertia increases, the nature of the order-disorder phase transition is changed from a continuous second-order transition to a discontinuous, or an explosive first-order one. For the latter case, a clear hysteresis region appears in which the order and disordered phases are coexisting. In particular, a relevant phenomenon of inertia-induced first-order synchronization transition was found in a second-order Kuramoto model [38,39]. A counterintuitive “slower is faster” effect of the inertia on ordering dynamics of the voter model was reported in Ref. [40].

**II. MODEL**

We first describe the original MV model defined on underlying networks. Each node is assigned to a binary spin variable  $\sigma_i \in \{+1, -1\}$  ( $i = 1, \dots, N$ ). In each step, a node  $i$  is randomly chosen and tends to align with the local neighborhood majority but with a noise parameter  $f$  giving the

\*chenhshf@ahu.edu.cn

†hzhlj@ustc.edu.cn

‡Juergen.Kurths@pik-potsdam.de

probability of misalignment. In this way, the single spin-flip probability from  $\sigma_i$  to  $-\sigma_i$  can be written as

$$w(\sigma_i) = \frac{1}{2}[1 - (1 - 2f)\sigma_i S(\Theta_i)], \quad (1)$$

with

$$\Theta_i = \sum_{j=1}^N a_{ij}\sigma_j, \quad (2)$$

where  $S(x) = \text{sgn}(x)$  if  $x \neq 0$  and  $S(0) = 0$ . The elements of the adjacency matrix of the underlying network are defined as  $a_{ij} = 1$  if nodes  $i$  and  $j$  are connected and  $a_{ij} = 0$  otherwise.

In the original MV model, the state update of each node depends exclusively on the states of its neighboring nodes, regardless of its own state. Here we incorporate the inertial effect into the original model by replacing Eq. (2) with

$$\Theta_i = (1 - \theta) \sum_{j=1}^N a_{ij}\sigma_j/k_i + \theta\sigma_i, \quad (3)$$

where  $k_i = \sum_{j=1}^N a_{ij}$  is the degree of node  $i$  and  $\theta \in [0, 0.5]$  is a parameter controlling the weight of the inertia. The larger the value of  $\theta$  is, the larger the inertia of the system is. For  $\theta = 0$ , we recover the original MV model where no inertia exists. For  $\theta = 0.5$ , our model is dominated by inertia other than the random spin flip with probability  $f$ . In this case, there is no spontaneous magnetization to appear. We should note that the generalization of the inertial MV model from two states to multiple states is straightforward, which is discussed in the Appendix.

### III. RESULTS

The phase behavior of the system can be characterized by the average magnetization per node  $m = \sum_{i=1}^N \sigma_i/N$ ;  $m = 0$  for the disordered phase and  $m \neq 0$  for the ordered phase. By Monte Carlo (MC) simulations, Fig. 1 shows the absolute

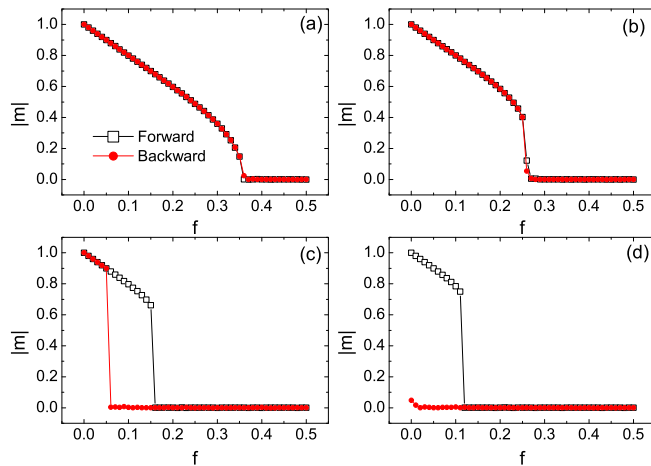


FIG. 1. Absolute magnetization  $|m|$  as a function of noise intensity  $f$  on ER random networks with different inertia parameter  $\theta$ : (a)  $\theta = 0$ , (b)  $\theta = 0.2$ , (c)  $\theta = 0.3$ , and (d)  $\theta = 0.35$ . The squares and circles correspond to forward and backward simulations, respectively. The network parameters are  $N = 10000$  and  $\langle k \rangle = 20$ .

value of  $m$  as a function of  $f$  for several different values of  $\theta$  on Erdős-Rényi (ER) random networks (RNs) with the size  $N = 10000$  and the average degree  $\langle k \rangle = 20$ . The simulation results are obtained by performing forward and backward simulations, respectively. The former is done by calculating the stationary value of  $m$  as  $f$  increases from 0 to 0.5 in steps of 0.01 and using the final configuration of the last simulation run as the initial condition of the next run, while the latter is performed by decreasing  $f$  from 0.5 to 0 with the same step. For  $\theta = 0$ , the results on the forward and backward simulations coincide, implying that the order-disorder transition is a continuous second-order phase transition that is the main feature of the original MV model. For  $\theta = 0.2$ , although the transition becomes sharper and the transition point shifts to a smaller value of  $f$ , the forward and backward simulations still coincide. Strikingly, for  $\theta = 0.3$ , one can see that as  $f$  increases,  $|m|$  abruptly jumps from nonzero to zero at  $f = f_{cF}$ , which shows that a sharp transition takes place for the order-disorder transition [Fig. 1(c)]. On the other hand, the curve corresponding to the backward simulations also shows a sharp transition from the disordered phase to the ordered phase at  $f = f_{cB}$ . These two sharp transitions occur at different values of  $f$ , leading to a clear hysteresis loop with respect to the dependence of  $|m|$  on  $f$ . Such a feature indicates that a discontinuous first-order order-disorder transition arises due to the effect of inertia. By further increasing  $\theta$  to  $\theta = 0.35$ ,  $f_{cF}$  shifts to a smaller value and  $f_{cB}$  decreases to zero, but the nature of a discontinuous phase transition is still present.

Within the hysteresis region, we observe phase flips between the ordered phase and the disordered one for a rather small network size  $N$ , as shown in Fig. 2(a) by a long time series of  $m$  in an ER network of  $N = 500$ . We show in Figs. 2(b)–2(d) the probability density function (PDF) of  $m$  for three distinct  $f$  chosen from the hysteresis region. On the one hand, all of them are multimodal distributions with a peak at  $m = 0$  and two other peaks symmetrically located at both sides of it. On the other hand, with the increase of  $f$  the peak at  $m = 0$  becomes higher, implying that the disordered phase becomes more stable. To calculate the transition rates between the ordered and disordered phases, a long-time simulation is necessary. However, for a larger network size the

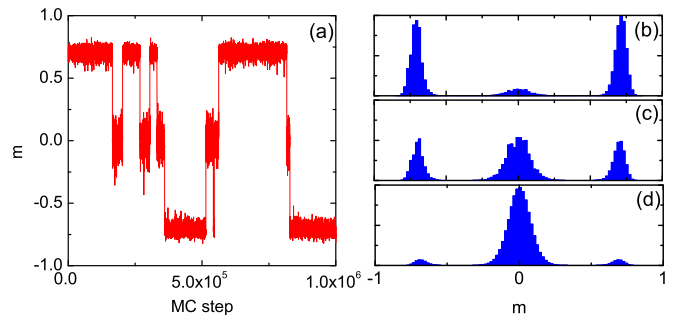


FIG. 2. (a) Time series of magnetization  $m$  show the transition events between ordered and disordered phases within the hysteresis region. Also shown is the PDF of  $m$  for (b)  $f = 0.136$ , (c)  $f = 0.138$ , and (d)  $f = 0.14$ . The other parameters are  $\theta = 0.3$ ,  $N = 500$ , and  $\langle k \rangle = 20$ .

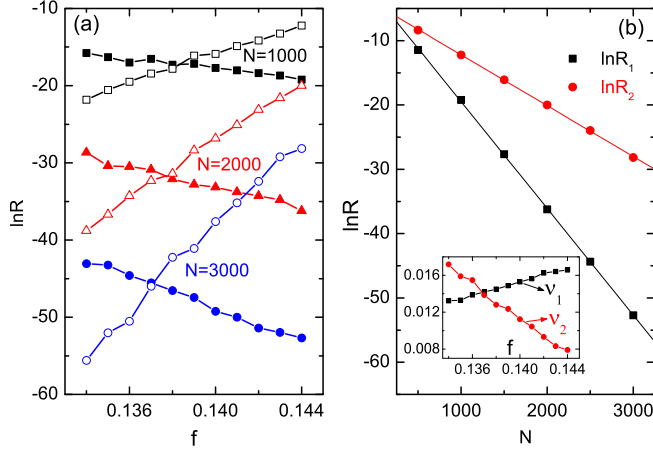


FIG. 3. (a) Logarithm of transition rates  $\ln R$  as a function of  $f$  for different  $N$ . Closed symbols correspond to the transition rate from the disordered state to the ordered state and open symbols to the transition rate from the ordered state to the disordered state. (b) Logarithm of transition rates  $\ln R$  as a function of  $N$  for  $f = 0.144$ . The lines indicate the linear fitting  $\ln R_{1(2)} \sim -\nu_{1(2)}N$ . The inset shows the fitting exponents  $\nu_{1(2)}$  as a function of  $f$ .

transition rates are extremely low and brute-force simulation is prohibitively expensive. To overcome this difficulty, we have used a rare-event simulation method: forward flux sampling (FFS) [41]. The FFS method uses a series of interfaces in phase space between the initial and final states to force the system from the initial state to the final state in a ratchetlike manner, which has been widely used to calculate rate constants and transition paths for rare events in various equilibrium and nonequilibrium systems [42]. In Fig. 3(a) we show the transition rate  $R_1$  from disordered to ordered phases and the inverse transition rate  $R_2$  as a function of  $f$  for several different  $N$ . Here  $R_1$  is a decreasing function of  $f$  and  $R_2$  is an increasing function of  $f$ . The intersection point of both curves determines the location at which the ordered and disordered phases are equally stable. As  $N$  increases, the intersection point slightly shifts to a smaller value. In Fig. 3(b) we show the transition rates as a function of  $N$  at  $f = 0.144$ . Obviously, both  $R_1$  and  $R_2$  decrease exponentially with  $N$ ,  $R_{1(2)} \sim \exp(-\nu_{1(2)}N)$  with the exponents  $\nu_{1(2)}$ , implying that the disordered and ordered phases are coexisting in the thermodynamic limit. In the inset of Fig. 3(b) we give the fitting exponents  $\nu_{1(2)}$  as a function of  $f$  and they clearly exhibit the different variation trends with  $f$ .

In the following we will present a mean-field theory to understand the simulation results. We first define  $m_k$  as the average magnetization of a node of degree  $k$  and  $\tilde{m}$  as the average magnetization of a randomly chosen nearest-neighbor node. For uncorrelated networks, the probability that a randomly chosen nearest-neighbor node has degree  $k$  is  $kP(k)/\langle k \rangle$ , where  $P(k)$  is the degree distribution defined as the probability that a node chosen at random has degree  $k$  and  $\langle k \rangle$  is the average degree [1]. Thus,  $m_k$  and  $\tilde{m}$  satisfy the relation

$$\tilde{m} = \sum_k k P(k) m_k / \langle k \rangle. \quad (4)$$

For an up-spin node  $i$  of degree  $k$ , the probability that its local field is positive can be written as the cumulative binomial distribution

$$P_{>}^+ = \sum_{n=\lceil n_k^+ \rceil}^k \left(1 - \frac{1}{2} \delta_{n, n_k^+}\right) C_k^n p_{\uparrow}^n p_{\downarrow}^{k-n}. \quad (5)$$

Here  $p_{\uparrow(\downarrow)} = (1 \pm \tilde{m})/2$  is the probability that a randomly chosen nearest-neighbor node has a +1 (-1) state,  $\lceil \cdot \rceil$  is the ceiling function,  $\delta$  is the Kronecker symbol,  $C_k^n = k!/(n!(k-n)!) are the binomial coefficients, and  $n_k^+ = (1 - 2\theta)k/2(1 - \theta)$  is the number of up-spin neighbors of node  $i$  satisfying  $\Theta_i = 0$ . Similarly, we can write the probability that the local field of a down-spin node of degree  $k$  is positive as$

$$P_{>}^- = \sum_{n=\lceil n_k^- \rceil}^k \left(1 - \frac{1}{2} \delta_{n, n_k^-}\right) C_k^n p_{\uparrow}^n p_{\downarrow}^{k-n}, \quad (6)$$

where  $n_k^- = k - n_k^+ = k/2(1 - \theta)$ .

Furthermore, the spin-flip probability  $\omega_k^+$  of an up-spin node of degree  $k$  can be expressed as the sum of two parts

$$\omega_k^+ = f P_{>}^+ + (1 - f)(1 - P_{>}^+), \quad (7)$$

where the first part is that the local field of the node is positive and the minority rule is applied and the other one is that the local field of the node is negative and the majority rule is applied. Likewise, we can write the spin-flip probability of a down-spin node of degree  $k$  as

$$\omega_k^- = f(1 - P_{>}^-) + (1 - f)P_{>}^-. \quad (8)$$

Thus, the rate equations for  $m_k$  are

$$\dot{m}_k = -\left(\frac{1 + m_k}{2}\right) \omega_k^+ + \left(\frac{1 - m_k}{2}\right) \omega_k^-. \quad (9)$$

In the steady state  $\dot{m}_k = 0$ , we have

$$m_k = \frac{\omega_k^- - \omega_k^+}{\omega_k^+ + \omega_k^-}. \quad (10)$$

Inserting Eq. (10) into Eq. (4), we get a self-consistent equation of  $\tilde{m}$ ,

$$\tilde{m} = \Psi(\tilde{m}), \quad (11)$$

with

$$\Psi(\tilde{m}) = \sum_k \frac{k P(k)}{\langle k \rangle} \frac{\omega_k^- - \omega_k^+}{\omega_k^+ + \omega_k^-}.$$

Since  $P_{>}^+ + P_{>}^- = 1$  and  $\omega_k^+ = \omega_k^-$  at  $\tilde{m} = 0$ , one can easily check that  $\tilde{m} = 0$  is always a stationary solution of Eq. (11). This solution corresponds to a disordered phase. The other possible solutions can be obtained by numerically iterating Eq. (11). Once  $\tilde{m}$  is found, we can immediately calculate  $m_k$  by Eq. (10) and the average magnetization per node by  $m = \sum_k P(k) m_k$ .

By a detailed numerical calculation for Eq. (11) on the ER RN with the Poisson degree distribution  $P(k) = \langle k \rangle^k e^{-\langle k \rangle} / k!$  and the average degree  $\langle k \rangle = 20$ , we find that the critical value of  $\theta$  is  $\theta_c = 0.23$ . In Fig. 4 we show the theoretical results on  $|\tilde{m}|$  as a function of  $f$  for three typical values of  $\theta$ :  $\theta = 0.15, 0.23$ , and  $0.3$ . For  $\theta < \theta_c$ , the ordered-disordered phase transition is of continuous second-order type. For

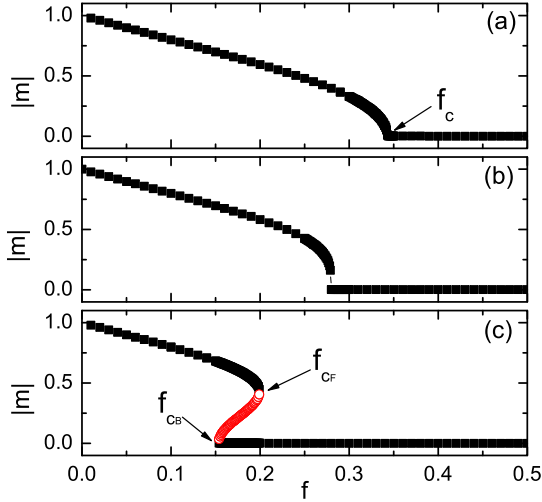


FIG. 4. Theoretical result of  $|m|$  as a function of  $f$  for three typical values of  $\theta$ : (a)  $\theta = 0.15$ , (b)  $\theta = 0.23$ , and (c)  $\theta = 0.3$ . In (c) circles within the hysteresis region indicate the unstable solution.

$\theta > \theta_c$ , the phase transition is of discontinuous first-order type and a clear hysteresis loop appears. As  $\theta$  decreases from above, the hysteresis loop shrinks until it vanishes at  $\theta = \theta_c$ .

At the critical noises  $f_{cF}$  and  $f_{cB}$ , the susceptibilities  $\tilde{\chi} = \partial\tilde{m}/\partial f$  are diverging. According to Eq. (11), the condition is equivalent to

$$\begin{aligned} \frac{\partial\Psi}{\partial\tilde{m}} = (1-2f) \sum_k \frac{kP(k)}{\langle k \rangle} & \left[ (\omega_k^- + \omega_k^+)^{-1} \left( \frac{\partial P_{>}^+}{\partial\tilde{m}} + \frac{\partial P_{>}^-}{\partial\tilde{m}} \right) \right. \\ & \left. + (\omega_k^- - \omega_k^+) (\omega_k^- + \omega_k^+)^{-2} \left( \frac{\partial P_{>}^+}{\partial\tilde{m}} - \frac{\partial P_{>}^-}{\partial\tilde{m}} \right) \right] = 1. \end{aligned} \quad (12)$$

Here  $\partial P_{>}^{\pm}/\partial\tilde{m}$  can be derived from Eqs. (5) and (6),

$$\begin{aligned} \frac{\partial P_{>}^{\pm}}{\partial\tilde{m}} = & \left( 1 - \frac{1}{2} \delta_{n_k^{\pm}, \lceil n_k^{\pm} \rceil} \right) \mathbb{P}(\lceil n_k^{\pm} \rceil; k) \\ & + \frac{1}{2} \delta_{n_k^{\pm}, \lceil n_k^{\pm} \rceil} \mathbb{P}(\lceil n_k^{\pm} \rceil + 1; k), \end{aligned} \quad (13)$$

where the function  $\mathbb{P}(n; k)$  is defined as

$$\mathbb{P}(n; k) = \frac{1}{2} k C_{k-1}^{n-1} p_{\uparrow}^{n-1} p_{\downarrow}^{k-n}. \quad (14)$$

For any given  $\theta$ ,  $f_{cF}$  and  $f_{cB}$  are determined by numerically solving Eqs. (11) and (12). In fact,  $f_{cB}$  can be obtained more conveniently, since  $f_{cB}$  corresponds to the point at which the trivial solution  $\tilde{m} = 0$  loses its stability. Therefore,  $f_{cB}$  is determined solely by Eq. (12). At  $\tilde{m} = 0$ , Eq. (12) can be reduced to

$$\frac{\partial\Psi}{\partial\tilde{m}} \Big|_{\tilde{m}=0} = (1-2f_{cB}) \sum_k \frac{kP(k)}{\langle k \rangle} \left[ \frac{\partial P_{>}^+}{\partial\tilde{m}} + \frac{\partial P_{>}^-}{\partial\tilde{m}} \right]_{\tilde{m}=0} \left[ \frac{1}{\omega_k^- + \omega_k^+} \right]_{\tilde{m}=0} = 1. \quad (15)$$

In Fig. 5 we plot the phase diagram in the  $\theta$ - $f$  plane for three types of networks [from left to right, random degree (RD) RNs, ER RNs, and Barabási-Albert (BA) scale-free networks (SFNs)] with two different average degrees:  $\langle k \rangle = 20$  (top panels) and  $\langle k \rangle = 40$  (bottom panels). The lines and symbols indicate the theoretical and simulation results, respectively. For RD RNs, each node has the same degree  $k$ , which is a typical representation of degree homogeneous networks. For BA SFNs, its degree distribution follows a power-law function with the exponent  $-3$ , which is typical for degree heterogeneous networks. Clearly, there is no essential difference in the phase diagrams for different network types and average degree. The phase diagram is divided into three regions by  $f_{cF}$  and  $f_{cB}$ . In the region below  $f_{cB}$ , the system is ordered. In the region

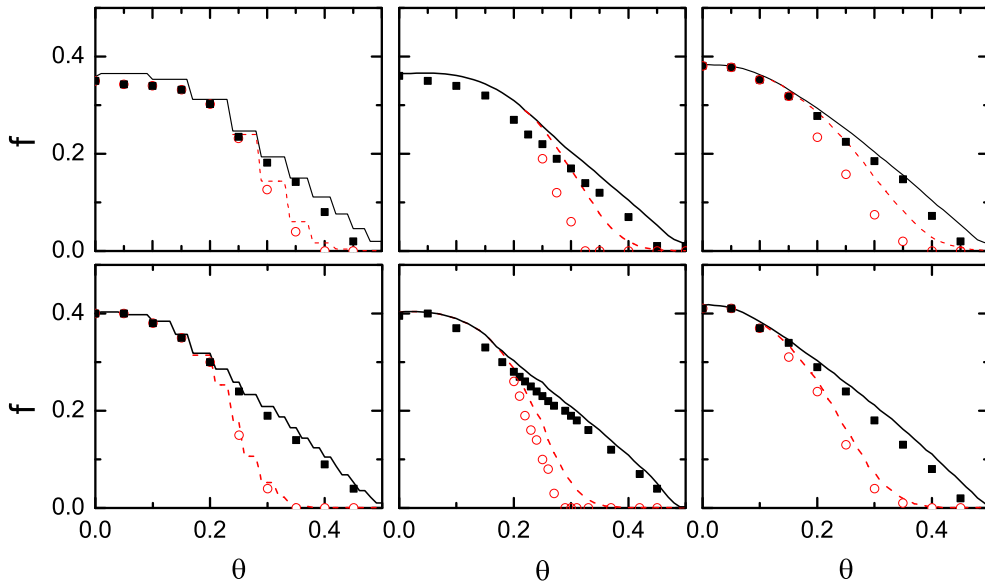


FIG. 5. Phase diagram in the  $\theta$ - $f$  plane for three types of networks with two different average degrees,  $\langle k \rangle = 20$  (top panels) and  $\langle k \rangle = 40$  (bottom panels) (from left to right): RD RNs, ER RNs, and BA SFNs. Lines and symbols correspond to the theoretical and simulation results, respectively. The  $f_{cF}$  are indicated by solid lines and squares and  $f_{cB}$  by dashed lines and circles. The sizes of all the networks are the same:  $N = 10000$ .

above  $f_{cF}$ , the system is disordered. Between  $f_{cF}$  and  $f_{cB}$ , the region is of hysteresis with a disordered phase and two ordered phases of up-down symmetry. As expected, for networks with a larger average degree the mean-field theory provides a better prediction for the simulation results. Although there exist obvious differences for a smaller network connectivity, the theory and simulations are qualitatively consistent.

#### IV. CONCLUSION

We have investigated the order-disorder phase transition in a MV model with inertia, where the inertia is introduced into the state-updating dynamics of nodes by considering the state of each node itself besides the states of its neighboring nodes. We mainly find that in contrast to a continuous second-order phase transition in the original MV model, the inertial MV model undergoes a discontinuous first-order phase transition when the inertia is large enough. In the hysteresis region of the first-order phase transition, a disordered phase and two symmetric ordered phases are coexisting. The transition rates between the disordered and ordered phases have been calculated by a highly efficient rare-event sampling method, forward flux sampling. A mean-field theory provides an analytical understanding for this interesting phenomenon. Since behavioral inertia is an essential characteristic of human beings and animal groups, our work may provide insight into the transition phenomena from disorder to order, such as the emergence of a consensus and decision making [43,44], as well as the spontaneous formation of a common language or culture [7,45]. Finally, we expect further investigations of the inertial effect in other dynamical systems.

#### ACKNOWLEDGMENTS

This work was supported by the National Natural Science Foundation of China (Grants No. 11205002, No. 61473001, No. 11475003, and No. 21473165), the Key Scientific Research Fund of the Anhui Provincial Education Department (Grant No. KJ2016A015), and the “211” Project of Anhui University (Grant No. J01005106).

#### APPENDIX: INERTIAL MV MODEL WITH MULTIPLE STATES

The original two-state MV model has been previously extended to three states [46,47] and to an arbitrary number of states [48]. Here we describe the MV model with arbitrary multiple states. Each node  $i$  can be in any of  $p$  states:  $\sigma_i \in \{1, \dots, q\}$ . The proportion of neighboring nodes of node  $i$  in any state  $\alpha \in \{1, \dots, q\}$  can be calculated as  $w_\alpha = \sum_{j=1}^N a_{ij} \delta_{\alpha, \sigma_j} / k_i$ , where  $a_{ij}$  are the elements of adjacency matrix of the underlying network,  $k_i$  is the degree of node  $i$ , and  $\delta_{\alpha, \beta} = 1$  if  $\alpha = \beta$  and  $\delta_{\alpha, \beta} = 0$  otherwise. With probability  $1 - f$ , node  $i$  takes the same value as the majority spin, i.e.,  $\sigma_i = \alpha|_{w_\alpha = \max\{w_1, \dots, w_q\}}$ . With supplementary probability  $f$ , node  $i$  takes the same value as the minority spin, i.e.,  $\sigma_i = \alpha|_{w_\alpha = \min\{w_1, \dots, w_q\}}$ . If there are more than two possible states in the majority spin or in the minority spin, we randomly choose one of them. The inertial MV (IMV) model with arbitrary multiple states is immediately defined by replacing

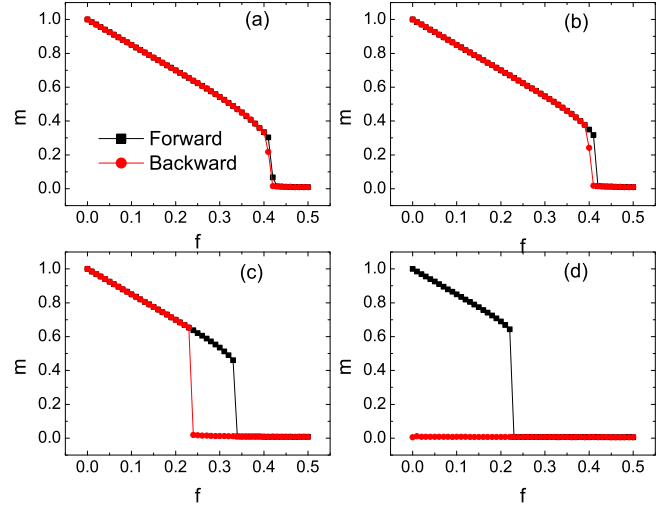


FIG. 6. The  $q = 3$  state IMV model. The order parameter  $m$  is plotted as a function of noise intensity  $f$  on ER random networks with different inertia factor  $\theta$ : (a)  $\theta = 0$ , (b)  $\theta = 0.1$ , (c)  $\theta = 0.2$ , and (d)  $\theta = 0.3$ . The squares and circles correspond to forward and backward simulations, respectively. The network parameters are  $N = 10000$  and  $\langle k \rangle = 20$ .

the above  $w_\alpha$  with  $w_\alpha = (1 - \theta) \sum_{j=1}^N a_{ij} \delta_{\alpha, \sigma_j} / k_i + \theta \delta_{\alpha, \sigma_i}$ , where  $\theta$  is the inertial factor. If  $q = 2$ , we recover the two-state inertial MV model discussed in the main text. To characterize the collective behavior of the model, we define the order parameter as  $m = |N^{-1} \sum_{j=1}^N e^{I2\pi\sigma_j/q}|$ , with the imaginary unit  $I$ ;  $m > 0$  corresponds to an ordered state and  $m = 0$  to a disordered state.

In Fig. 6 we plot the order parameter  $m$  as a function of noise intensity  $f$  on ER random networks with different  $\theta$  for  $q = 3$ . Qualitatively, the main conclusion for  $q = 3$  is the same

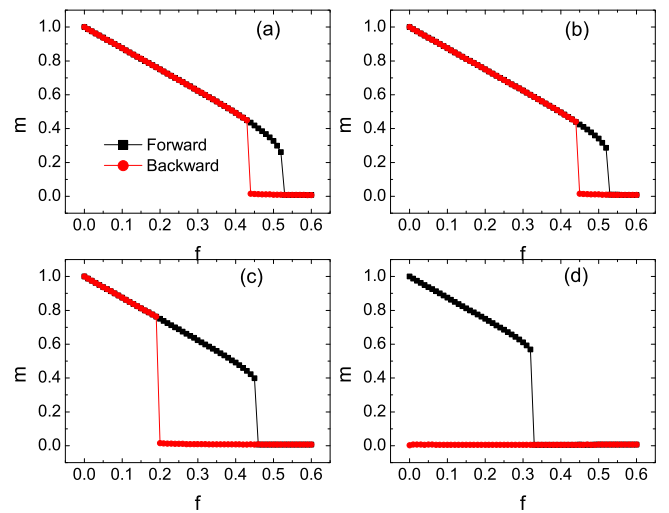


FIG. 7. The  $q = 5$  state IMV model. The order parameter  $m$  is plotted as a function of noise intensity  $f$  on ER random networks with different inertia factor  $\theta$ : (a)  $\theta = 0$ , (b)  $\theta = 0.1$ , (c)  $\theta = 0.2$ , and (d)  $\theta = 0.3$ . The squares and circles correspond to forward and backward simulations, respectively. The network parameters are  $N = 10000$  and  $\langle k \rangle = 20$ .

as the case of  $q = 2$  shown in the main text. In the absence of the inertia, although  $m$  has a slight jump at the order-disorder phase transition, the two curves corresponding to forward and backward simulations almost coincide. If the inertia is large enough, the transition becomes a discontinuous or an explosive

type [Figs. 6(c) and 6(d)]. In Fig. 7 we show the results of the  $q = 5$  state IMV model. The model exhibits a discontinuous order-disorder transition even if the inertia is absent. When the inertia is added, the hysteresis region is enlarged [Figs. 7(c) and 7(d)].

- 
- [1] S. N. Dorogovtsev, A. V. Goltsev, and J. F. F. Mendes, *Rev. Mod. Phys.* **80**, 1275 (2008).
- [2] R. Cohen, K. Erez, D. ben-Avraham, and S. Havlin, *Phys. Rev. Lett.* **85**, 4626 (2000).
- [3] D. S. Callaway, M. E. J. Newman, S. H. Strogatz, and D. J. Watts, *Phys. Rev. Lett.* **85**, 5468 (2000).
- [4] R. Pastor-Satorras, C. Castellano, P. Van Mieghem, and A. Vespignani, *Rev. Mod. Phys.* **87**, 925 (2015).
- [5] A. Arenas, A. Díaz-Guilera, J. Kurths, Y. Moreno, and C. Zhou, *Phys. Rep.* **469**, 93 (2008).
- [6] F. A. Rodrigues, T. K. Peron, P. Ji, and J. Kurths, *Phys. Rep.* **610**, 1 (2016).
- [7] C. Castellano, S. Fortunato, and V. Loreto, *Rev. Mod. Phys.* **81**, 591 (2009).
- [8] D. Achlioptas, R. M. D'Souza, and J. Spencer, *Science* **323**, 1453 (2009).
- [9] E. J. Friedman and A. S. Landsberg, *Phys. Rev. Lett.* **103**, 255701 (2009).
- [10] F. Radicchi and S. Fortunato, *Phys. Rev. Lett.* **103**, 168701 (2009).
- [11] Y. S. Cho, J. S. Kim, J. Park, B. Kahng, and D. Kim, *Phys. Rev. Lett.* **103**, 135702 (2009).
- [12] R. A. da Costa, S. N. Dorogovtsev, A. V. Goltsev, and J. F. F. Mendes, *Phys. Rev. Lett.* **105**, 255701 (2010).
- [13] P. Grassberger, C. Christensen, G. Bizhani, S.-W. Son, and M. Paczuski, *Phys. Rev. Lett.* **106**, 225701 (2011).
- [14] O. Riordan and L. Warnke, *Science* **333**, 322 (2011).
- [15] R. M. D'Souza and J. Nagler, *Nat. Phys.* **11**, 531 (2015).
- [16] S. V. Buldyrev, R. Parshani, G. Paul, H. E. Stanley, and S. Havlin, *Nature (London)* **464**, 1025 (2010).
- [17] R. Parshani, S. V. Buldyrev, and S. Havlin, *Phys. Rev. Lett.* **105**, 048701 (2010).
- [18] J. Gao, S. V. Buldyrev, S. Havlin, and H. E. Stanley, *Phys. Rev. Lett.* **107**, 195701 (2011).
- [19] J. Gómez-Gardeñes, S. Gómez, A. Arenas, and Y. Moreno, *Phys. Rev. Lett.* **106**, 128701 (2011).
- [20] I. Leyva, R. Sevilla-Escoboza, J. M. Buldú, I. Sendiña-Nadal, J. Gómez-Gardeñes, A. Arenas, Y. Moreno, S. Gómez, R. Jaimés-Reátegui, and S. Boccaletti, *Phys. Rev. Lett.* **108**, 168702 (2012).
- [21] P. Ji, T. K. DM. Peron, P. J. Menck, F. A. Rodrigues, and J. Kurths, *Phys. Rev. Lett.* **110**, 218701 (2013).
- [22] X. Zhang, S. Boccaletti, S. Guan, and Z. Liu, *Phys. Rev. Lett.* **114**, 038701 (2015).
- [23] J.-H. Zhao, H.-J. Zhou, and Y.-Y. Liu, *Nat. Commun.* **4**, 2412 (2013).
- [24] A. Majdandzic, B. Podobnik, S. V. Buldyrev, D. Y. Kenett, S. Havlin, and H. E. Stanley, *Nat. Phys.* **10**, 34 (2014).
- [25] L. Chen, F. Ghanbarnejad, W. Cai, and P. Grassberger, *Europhys. Lett.* **104**, 50001 (2013).
- [26] W. Cai, L. Chen, F. Ghanbarnejad, and P. Grassberger, *Nat. Phys.* **11**, 936 (2015).
- [27] L. Hébert-Dufresne and B. M. Althouse, *Proc. Natl. Acad. Sci. U.S.A.* **112**, 10551 (2015).
- [28] M. J. de Oliveira, *J. Stat. Phys.* **66**, 273 (1992).
- [29] L. F. C. Pereira and F. G. B. Moreira, *Phys. Rev. E* **71**, 016123 (2005).
- [30] F. W. S. Lima, A. Sousa, and M. Sumuor, *Physica A* **387**, 3503 (2008).
- [31] P. R. A. Campos, V. M. de Oliveira, and F. G. Brady Moreira, *Phys. Rev. E* **67**, 026104 (2003).
- [32] E. M. S. Luz and F. W. S. Lima, *Int. J. Mod. Phys. C* **18**, 1251 (2007).
- [33] T. E. Stone and S. R. McKay, *Physica A* **419**, 437 (2015).
- [34] F. W. S. Lima, *Int. J. Mod. Phys. C* **17**, 1257 (2006).
- [35] F. W. S. Lima and K. Malarz, *Int. J. Mod. Phys. C* **17**, 1273 (2006).
- [36] H. Chen, C. Shen, G. He, H. Zhang, and Z. Hou, *Phys. Rev. E* **91**, 022816 (2015).
- [37] A. Attanasi, A. Cavagna, L. D. Castello, I. Giardina, T. S. Grigera, A. Jelić, S. Melillo, L. Parisi, O. Pohl, E. Shen *et al.*, *Nat. Phys.* **10**, 691 (2014).
- [38] H.-A. Tanaka, A. J. Lichtenberg, and S. Oishi, *Phys. Rev. Lett.* **78**, 2104 (1997).
- [39] S. Gupta, A. Campa, and S. Ruffo, *Phys. Rev. E* **89**, 022123 (2014).
- [40] H.-U. Stark, C. J. Tessone, and F. Schweitzer, *Phys. Rev. Lett.* **101**, 018701 (2008).
- [41] R. J. Allen, P. B. Warren, and P. R. ten Wolde, *Phys. Rev. Lett.* **94**, 018104 (2005).
- [42] R. J. Allen, C. Valeriani, and P. R. ten Wolde, *J. Phys.: Condens. Matter* **21**, 463102 (2009).
- [43] V. Sood and S. Redner, *Phys. Rev. Lett.* **94**, 178701 (2005).
- [44] A. T. Hartnett, E. Schertzer, S. A. Levin, and I. D. Couzin, *Phys. Rev. Lett.* **116**, 038701 (2016).
- [45] C. Castellano, M. Marsili, and A. Vespignani, *Phys. Rev. Lett.* **85**, 3536 (2000).
- [46] D. F. F. Melo, L. F. C. Pereira, and F. G. B. Moreira, *J. Stat. Mech.* (2010) P11032.
- [47] F. Lima, *Physica A* **391**, 1753 (2012).
- [48] G. F. Li, H. S. Chen, F. Huang, and C. S. Shen, *J. Stat. Mech.* (2016) 073403.